

## **Supporting Information**

# **Carbon Nanohorn-Derived Graphene Nanotubes as a Platinum-Free Fuel Cell Cathode**

**Sreekuttan M. Unni<sup>‡</sup>, Rajith Illathvalappil<sup>‡</sup>, Siddheshwar N. Bhange<sup>‡</sup>,  
Hasna Puthenpediakkal<sup>‡</sup> and Sreekumar Kurungot<sup>\*‡</sup>**

<sup>‡</sup> Physical and Materials Chemistry Division, CSIR-National Chemical Laboratory, Pune,  
Maharashtra, India-411008, E-mail: [k.sreekumar@ncl.res.in](mailto:k.sreekumar@ncl.res.in)

<sup>‡</sup> Academy of Scientific and Innovative Research (AcSIR), CSIR-National Chemical  
Laboratory campus, Pune, Maharashtra, India-411008.

**Material Characterization:** FEI Technai G2 T30 operated at 300 kV and Quanta 200 3D FEI were used respectively for high resolution transmission electron microscopic (HR-TEM) and scanning electron microscopic (SEM) analysis. LabRam spectrometer (HJY, France) was used for Raman analysis with a laser wavelength of 632 nm. VGMicrotech Multilab ESCA 3000 spectrometer was used for X-ray photoelectron spectroscopic analysis by employing a monochromatic Mg  $K_{\alpha}$  X-ray source ( $h\nu = 1253.6$  eV). Brunauer-Emmet-Teller (BET) nitrogen adsorption-desorption experiment was performed on Quantachrome Quadrasorb automatic volumetric measurement system at 77 K using ultra pure nitrogen gas.

**Electrochemical Measurements:** Biologic electrochemical workstation (VMP3) was used for all the electrochemical measurements by using a three-electrode set-up. 0.1 M  $\text{HClO}_4$ , 0.5 M  $\text{H}_2\text{SO}_4$  and 0.1 M KOH were used as the electrolytes for the electrochemical measurements. Catalyst coated glassy carbon disc ( $0.196 \text{ cm}^2$  area, Pine Instruments, Inc.) was used as the working electrode. Different reference electrodes were used for the electrochemical measurements which are Ag/AgCl in 0.1 M  $\text{HClO}_4$ , Hg/HgSO<sub>4</sub> in 0.5 M  $\text{H}_2\text{SO}_4$  and Hg/HgO in 0.1 M KOH. For the purpose of comparison, all the potentials are converted to reference hydrogen electrode scale and used in the manuscript. A graphite rod was used as the counter electrode in all the three electrolytes. For the preparation of the catalyst ink, 10 mg of the catalyst was ultrasonically dispersed in a mixture of 1 ml of water-isopropyl alcohol (3:1) and 40  $\mu\text{l}$  of 5 wt. % Nafion solution for 1 h. 20  $\mu\text{l}$  of the catalyst slurry was drop coated on the glassy carbon electrode to get a total catalyst loading of  $1 \text{ mg cm}^{-2}$ . The glassy carbon electrode was polished using 0.05  $\mu\text{m}$  polishing alumina powder prior to drop coating of the catalyst ink. The catalyst ink was dried under an IR lamp for electrochemical analysis. Commercial Pt/C (40 wt. % from Johnson Matthey (Alpha Acessar)) was also studied for the comparison purpose. Catalyst ink for Pt/C was prepared by dispersing 10 mg of Pt/C in 1 ml of water and 40  $\mu\text{l}$  of Nafion (5 wt. % in water) using an

ultrasonic bath for 1 h. 5  $\mu\text{l}$  of the resulting ink was drop coated on the glassy carbon electrode in order to get a total Pt loading of  $100 \mu\text{g}_{\text{Pt}} \text{cm}^{-2}$ . Linear sweep voltammograms (LSVs) were recorded using a rotating disk electrode (RDE,  $0.196 \text{ cm}^2$ , Pine Instruments) at different electrode rotation speeds (400, 900, 1200, 1600 and 2500 rpm) in an oxygen saturated electrolyte with a scan rate of  $5 \text{ mV s}^{-1}$  at room temperature. For the durability analysis, accelerated durability test (ADT) was performed for 5000 cycles for FeGNT in all three electrolytes. CV was performed at  $100 \text{ mV s}^{-1}$  scan rate in between a potential window of 0.60 to 1.0 V under oxygen purging. LSV was taken before and after ADT at 1600 rpm with a scan rate of  $5 \text{ mV s}^{-1}$ .

Hydrogen peroxide percentage and number of electron transfer during the oxygen reduction reaction were measured using a rotating ring disc electrode (RRDE,  $0.245 \text{ cm}^2$ , Pine Instruments) voltammogram using the following equations:

$$n = 4 \times \frac{I_d}{I_d + \frac{I_r}{N}} \dots\dots\dots (1)$$

$$H_2O_2(\%) = 200 \times \frac{\frac{I_r}{N}}{I_d + \frac{I_r}{N}} \dots\dots\dots (2)$$

where,  $I_d$  is the disc current,  $I_r$  is the ring current, and  $N$  is the collection efficiency of the Pt ring (0.37).

### Single cell analysis

Nafion 212 membrane (DuPont, USA) was used as the proton exchange membrane. Initially the Nafion membrane was boiled in con.  $\text{HNO}_3$  for 1 h. This was followed by boiling the membrane in DI water, 1 M  $\text{H}_2\text{SO}_4$ , and DI water for another 1 h each. This pretreated membrane was used for the membrane electrode assembly (MEA) fabrication.

Electrodes were prepared by conventional brush coating method. For the cathode layer, a slurry of FeGNT and 20 wt. % Nafion (Dispersion in water, DuPont, USA) with a Nafion to carbon ratio (N/C) of 0.50 in isopropyl alcohol (IPA) was used. 2 mg cm<sup>-2</sup> of the catalyst loading was used on a gas diffusion layer (GDL, SGL CC, Germany). The anode electrode comprises of 40 wt. % Pt/C with a catalyst loading of 0.50 mg cm<sup>-2</sup> (N/C is 0.5). For comparison, the Pt/C cathode layer was also made with a Pt loading of 0.50 mg cm<sup>-2</sup> and an N/C ratio of 0.50.

MEA was prepared by keeping the Nafion membrane in between the cathode and anode followed by applying 0.25 ton pressure for 1 min. at 130 °C. 4 cm<sup>2</sup> is the active electrode area of the MEA. A standard test fixture (Fuel Cell Technologies Inc, USA) was used for the MEA performance analysis. The testing was done by using a fuel cell test station (Fuel Cell Technologies Inc, USA) by purging H<sub>2</sub> and O<sub>2</sub> with a flow rate of 50 sccm and 100 sccm respectively at the anode and cathode by maintaining a relative humidity of 100 % without applying back pressure and a cell operating temperature of 65 °C.

Table S1: Elemental composition of the different samples calculated from XPS.

Sample	C (At.%)	O (At.%)	N (At.%)	Fe (At.%)
FeGNT	88.87	7.64	3.10	0.39
FeNCNT	91.95	6.18	1.42	0.45
NCNH	88.67	10.26	1.10	0.00

Table S2: ORR activity comparison of FeGNT catalyst with reported non-precious metal catalyst in acidic medium

Catalyst	Preparation method	Electrolyte	Catalyst loading ( $\text{mg cm}^{-2}$ )	Onset potential (V vs RHE)	$E_{1/2}$ difference compared to Pt/C (mV)	reference
FeGNT	High temperature annealing of nanohorn, melamine and iron acetate	0.1 M $\text{HClO}_4$	1	0.9	150	Present study
FeGNT	High temperature annealing of nanohorn, melamine and iron acetate	0.5 M $\text{H}_2\text{SO}_4$	1	0.9	100	Present study
Fe-P-C <sup>1</sup>	High temperature annealing of phytic acid and Fe salt.	0.1 M $\text{HClO}_4$	0.039	0.84	~210	4
Fe-N-C catalyst <sup>2</sup>	Annealing of bidppz molecule and $\text{FeSO}_4$ at 800 °C	0.1 M $\text{HClO}_4$	0.1	~ 0.9	59	5
Carbon supported Fe-N catalysts <sup>3</sup>	Annealing of 2,4,6-tris(2-pyridyl)-1,3,5- triazine and Mohr's salt at 800 °C	0.5 M $\text{H}_2\text{SO}_4$	0.2	0.88	~140	6
Co and Fe loaded N doped carbon <sup>4</sup>	Annealing of 2,6-diaminopyridine in with Co and Fe salt at 700 °C in presence of $\text{NH}_3$	0.5 M $\text{H}_2\text{SO}_4$	0.5	0.84	110	7
Fe-N-C catalyst <sup>5</sup>	Annealing of carbendazim and $\text{FeCl}_3$ mixture with silica template at 800 °C	0.5 M $\text{H}_2\text{SO}_4$	0.6	~0.89	-----	8
Carbon Nanotube/ $\text{Fe}_3\text{C}$ nano particle <sup>6</sup>	annealing a mixture of PEG-PPG-PEG Pluronic P123, elamine, and $\text{Fe}(\text{NO}_3)_3$ at 800 °C in $\text{N}_2$ .	0.1 M $\text{HClO}_4$	1.2	0.88	~170	9
Fe-N-HCMS <sup>7</sup>	Silica template mediated annealing of EDA and iron	0.5 M $\text{H}_2\text{SO}_4$	0.25	0.80	~180	10

	nitrate					
Carbon nanotube-graphene complex <sup>8</sup>	Partial unzipping of carbon nanotube	0.1 M HClO <sub>4</sub>	0.5	~ 0.89	~ 100	11

Table S3: Electrochemical performance of the different catalysts including Pt/C in 0.1 M HClO<sub>4</sub>, 0.5 M H<sub>2</sub>SO<sub>4</sub> and 0.1 M KOH.

	Catalyst loading (mA cm <sup>-2</sup> )	Onset potential (V vs RHE)	Half wave potential (V vs RHE)	Tafel slope (mV decade <sup>-1</sup> )	Peroxide yield at 0.5 V vs RHE	Number of electron transfer at 0.5 V vs RHE
0.1 M HClO <sub>4</sub>						
Pt/C	0.1	0.99	0.87	66.84	2.80	3.95
FeGNT	1	0.90	0.71	77.40	5.30	3.89
FeNCNT	1	0.77	0.46	132.21	6.03	3.88
NCNH	1	0.80	0.49	146.04	6.02	3.88
0.5 M H <sub>2</sub> SO <sub>4</sub>						
Pt/C	0.1	0.98	0.85	64.23	1.47	3.97
FeGNT	1	0.90	0.75	77.94	2.30	3.95
FeNCNT	1	0.77	0.48	114.98	7.37	3.85
NCNH	1	0.71	0.41	211.19	7.37	3.85
0.1 M KOH						
Pt/C	0.1	1.00	0.86	91.00	3.45	3.94
FeGNT	1	1.00	0.85	84.84	5.01	3.90
FeNCNT	1	0.92	0.75	84.86	9.95	3.80
NCNH	1	0.92	0.75	91.14	3.01	3.94

**Table S4:** Half wave potential ( $E_{1/2}$ ) of FeGNT and Pt/C in 0.1 M HClO<sub>4</sub>, 0.5 M H<sub>2</sub>SO<sub>4</sub> and 0.1 M KOH before and after ADT.

Electrolyte	FeGNT		Pt/C	
	Before 5000 cycles, $E_{1/2}$ (V vs RHE)	After 5000 cycles, $E_{1/2}$ (V vs RHE)	Before 5000 cycles, $E_{1/2}$ (V vs RHE)	After 5000 cycles, $E_{1/2}$ (V vs RHE)
0.1 M HClO <sub>4</sub>	0.71	0.67	0.87	0.82
0.5 M H <sub>2</sub> SO <sub>4</sub>	0.75	0.73	0.00	0.00
0.1 M KOH	0.85	0.84	0.86	0.83

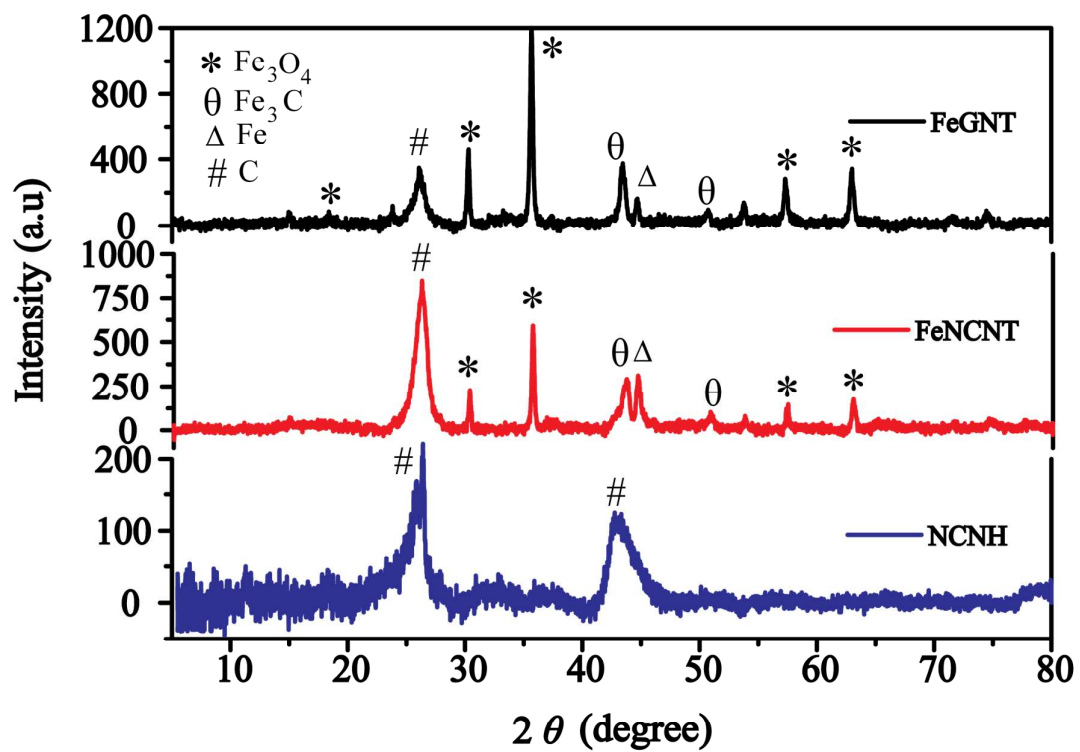


Figure S1. X-ray diffraction patterns of FeGNT, FeNCNT and NCNH.



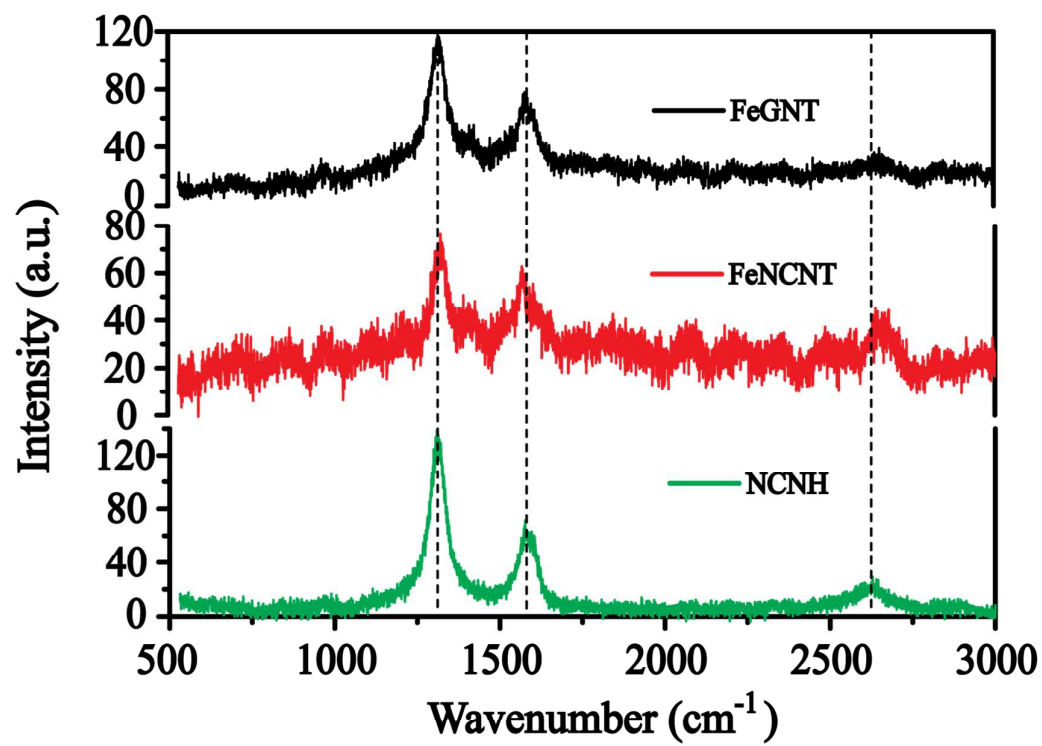


Figure S2. Raman analysis of FeGNT, FeNCNT and NCNH.

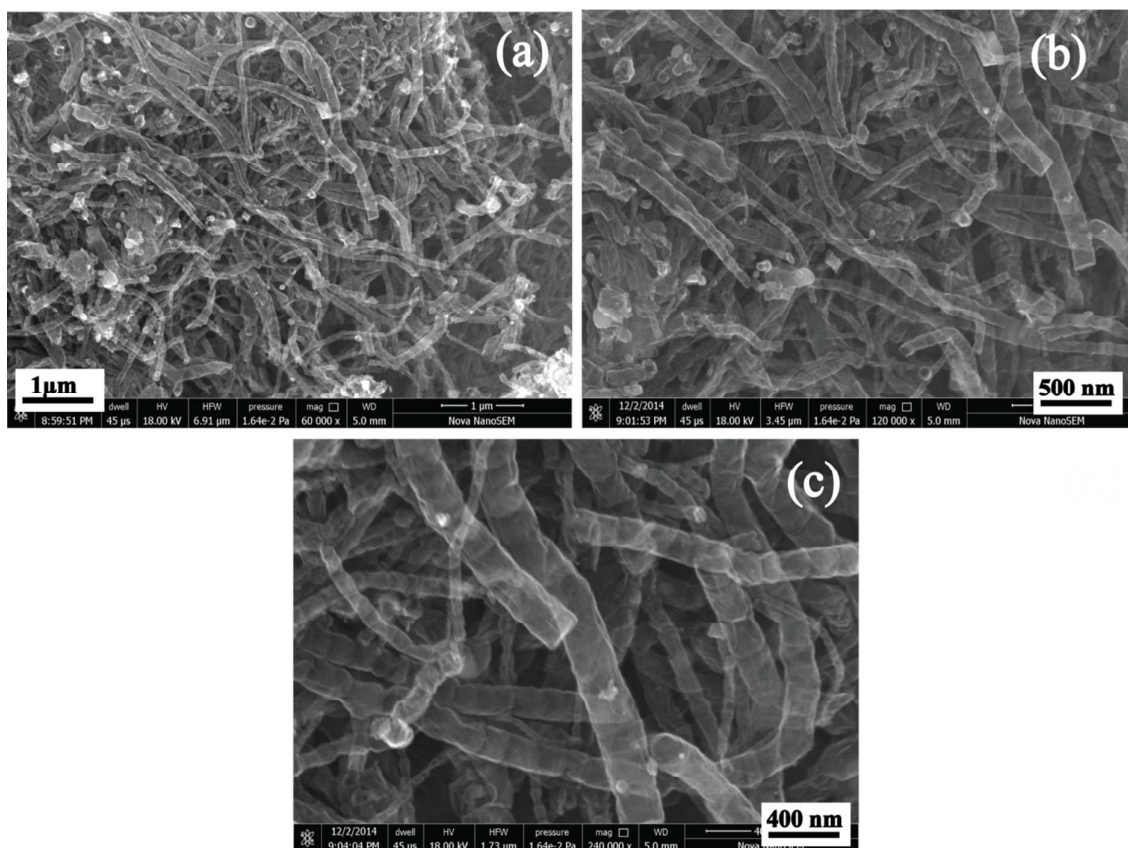


Figure S3. FE-SEM images of FeGNT at different magnifications ((a) scale: 1  $\mu\text{m}$ , (b) scale: 500 nm and (c) scale: 400nm).

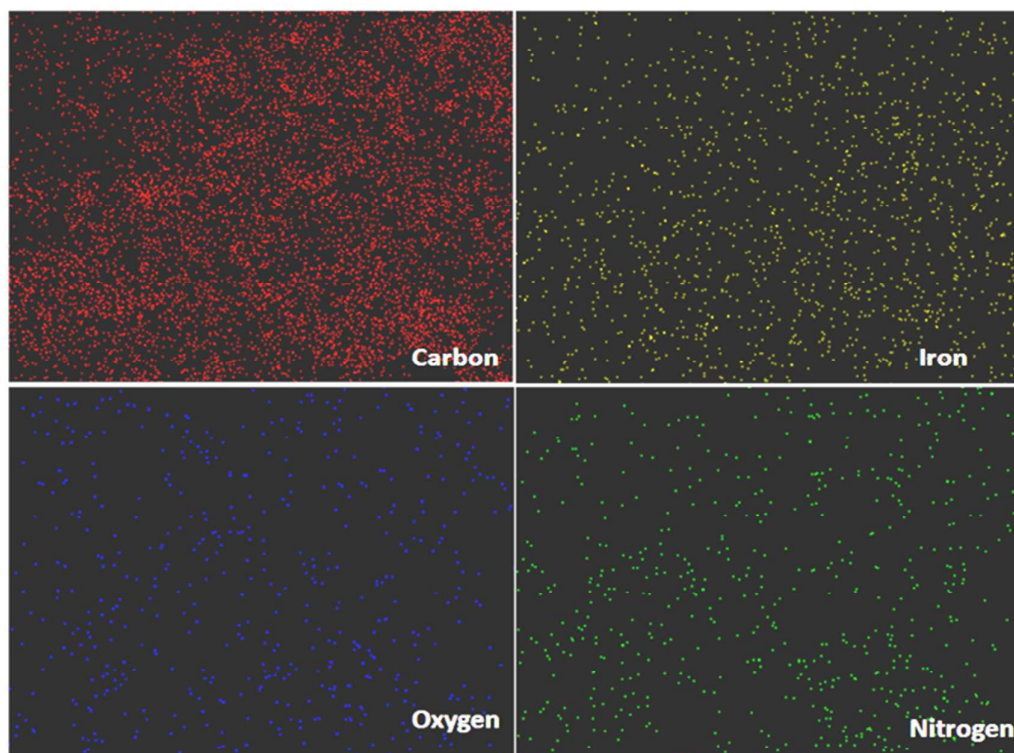


Figure S4. Elemental mapping of FeGNT using FE-SEM in a scale bar of 1  $\mu\text{m}$ .

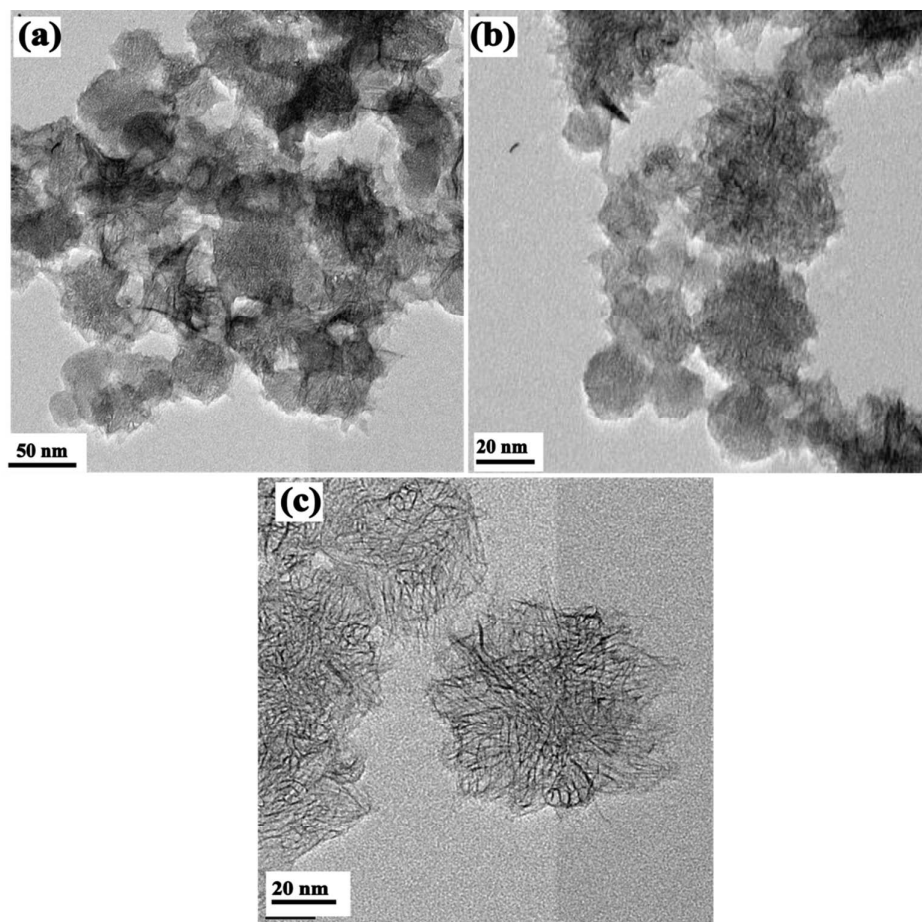


Figure S5. HR-TEM images of (a) FeCNO, (b) NCNH and (c) SWCNH.

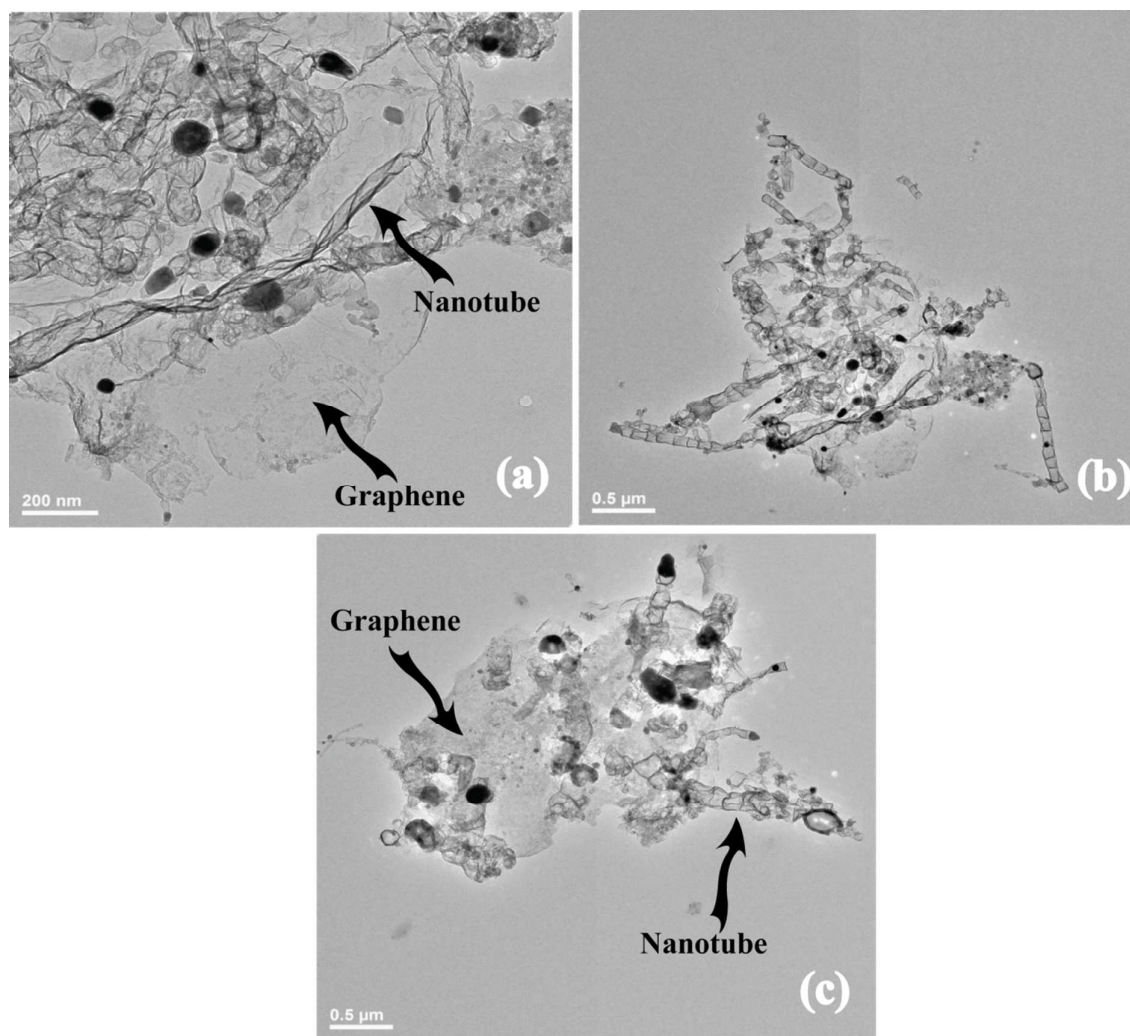
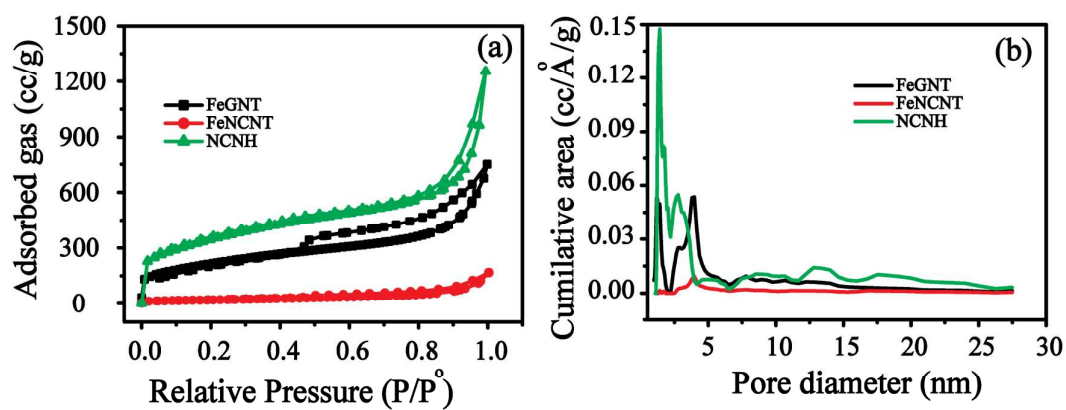
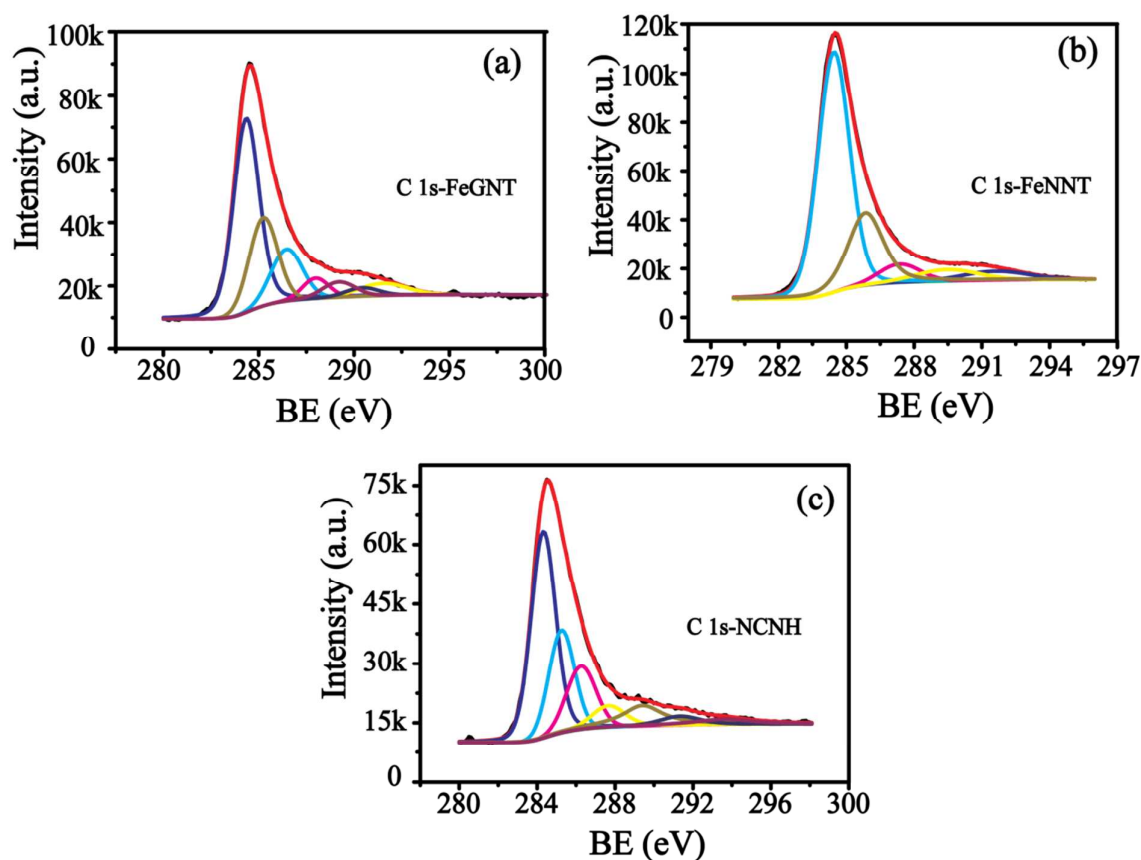


Figure S6. HR-TEM images of the nanotube grown on graphene sheets at different magnifications ((a), (b) and (c)).



**Figure S7.** (a) Nitrogen adsorption–desorption isotherms and (b) pore size distribution profiles of FeGNT, FeNCNT and NCNH.



**Figure S8.** Deconvoluted C1s spectra of (a) FeGNT, (b) FeNCNT and (c) NCNH.

Fitted C1s spectra of FeGNT show a peak at 284.34 eV corresponds to the  $sp^2$  carbon. Similarly, the peaks at 286.51 eV and 289.38 eV indicate different mode of C-O interactions in the carbon nanostructure.<sup>9</sup> The peak at 285.23 eV indicates the carbon nitrogen interaction where nitrogen is bonded with a  $sp^2$  carbon.<sup>10</sup> Similarly, the peak at 287.98 eV indicates the C-N bond where 'N' is attached to the  $sp^3$  carbon.<sup>10</sup> Similar peaks are also observed in FeNCNT and NCNH. Fitted C1s spectra of all the three catalysts give information about the nitrogen doping in the carbon matrix.



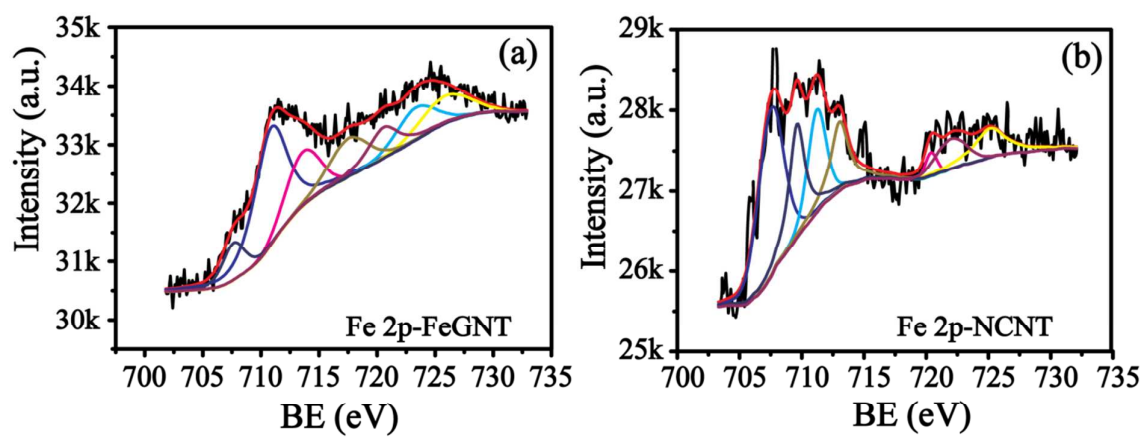


**Figure S9.** Deconvoluted Fe 2p spectra of (a) FeGNT and (b) FeNCNT.



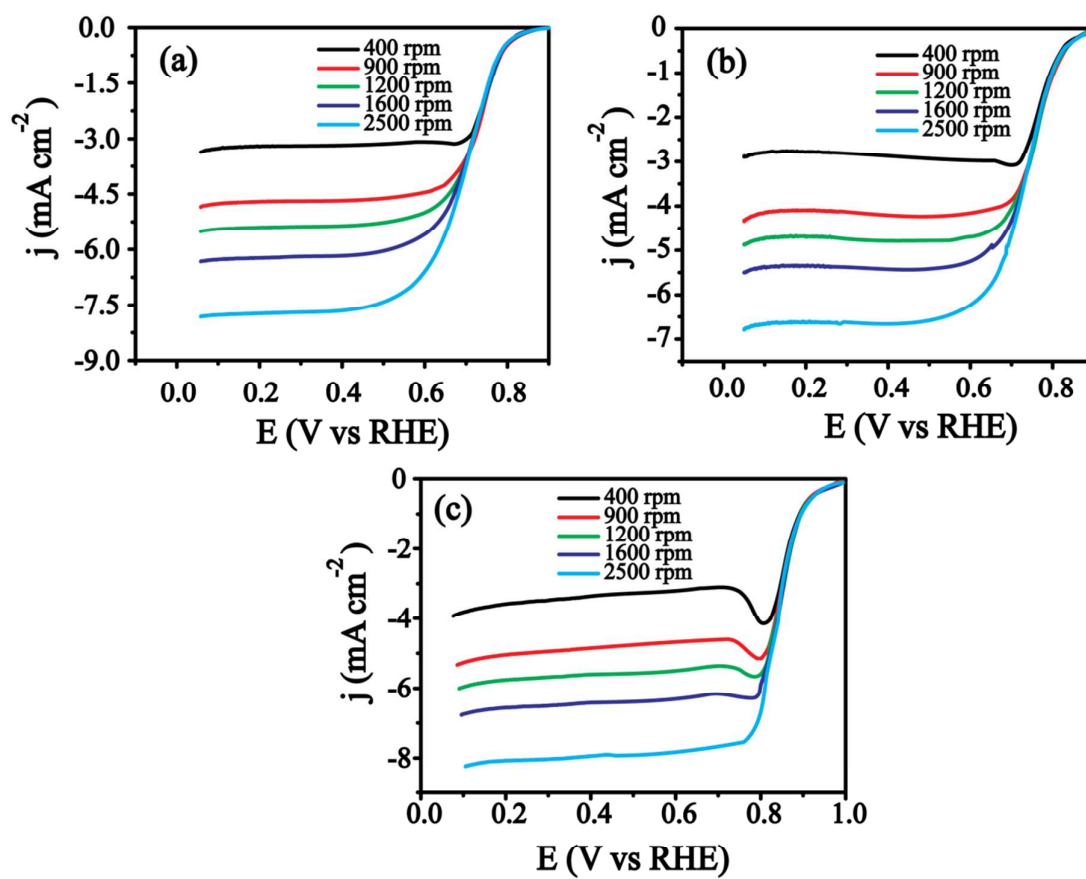


**Figure S10.** Linear sweep voltammograms of FeGNT at different electrode rotation rates in (a) 0.1 M HClO<sub>4</sub>, (b) 0.5 M H<sub>2</sub>SO<sub>4</sub> and (c) 0.1 M KOH.

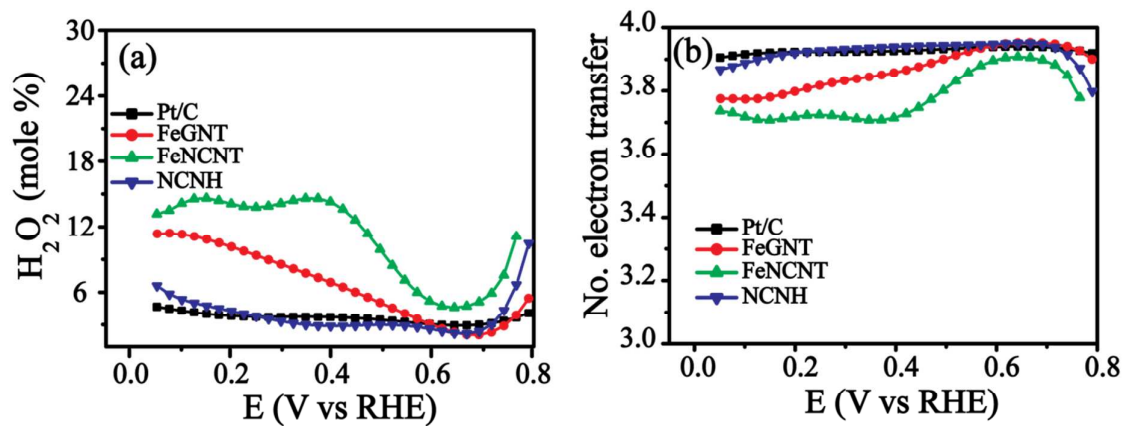


**Figure S11.** (a) Hydrogen peroxide yield and (b) number of electron transfer of the samples at different potentials in 0.1 M KOH calculated from RRDE.

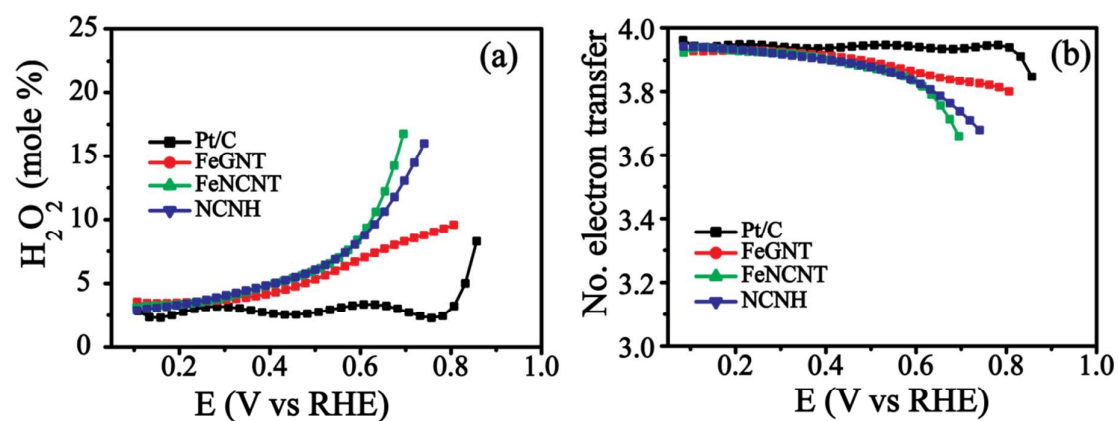


**Figure S12.** (a) Hydrogen peroxide yield and (b) number of electron transfer of the samples at different potentials in 0.1 M HClO<sub>4</sub> calculated from RRDE.

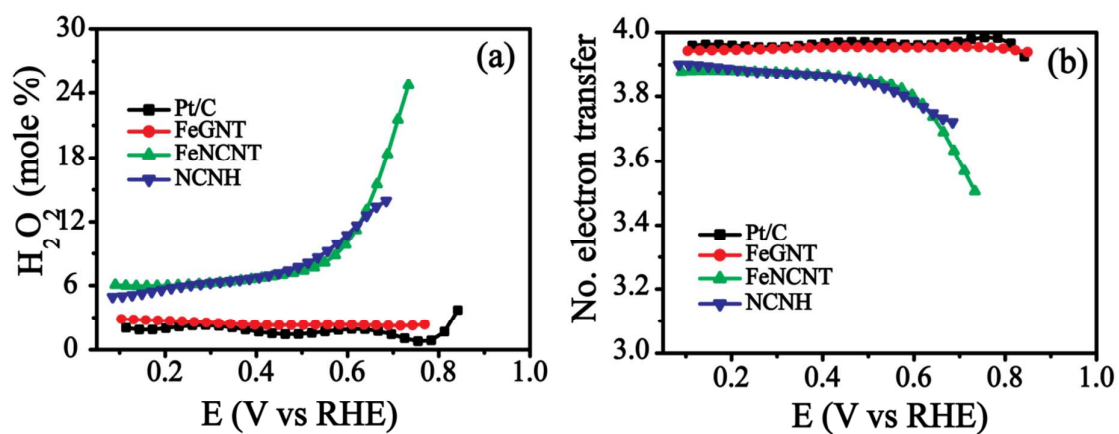


**Figure S13.** (a) Hydrogen peroxide yield and (b) number of electron transfer of the samples at different potentials in 0.5 M H<sub>2</sub>SO<sub>4</sub> calculated from RRDE.

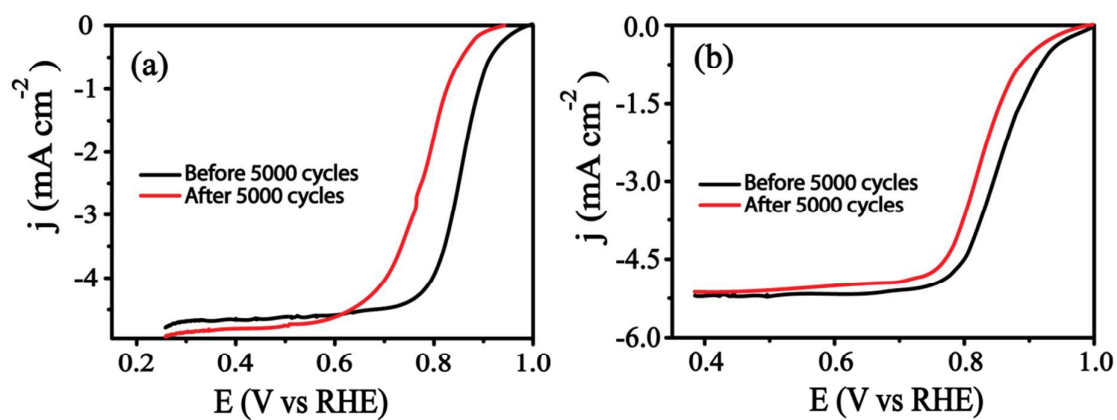


**Figure S14.** LSVs of Pt/C before and after ADT in (a) perchloric acid and (b) 0.1 M KOH with an electrode rotation rate of 1600 rpm and a scan rate of 5 mV s<sup>-1</sup>.

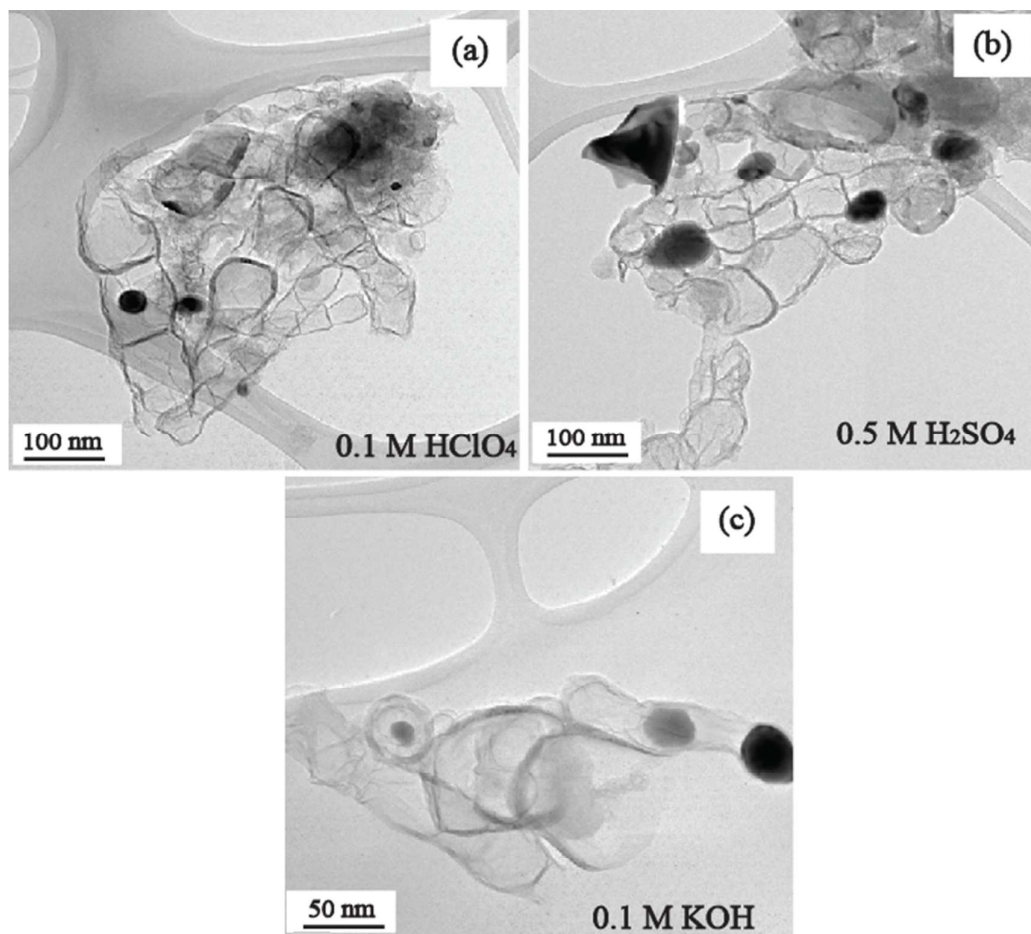
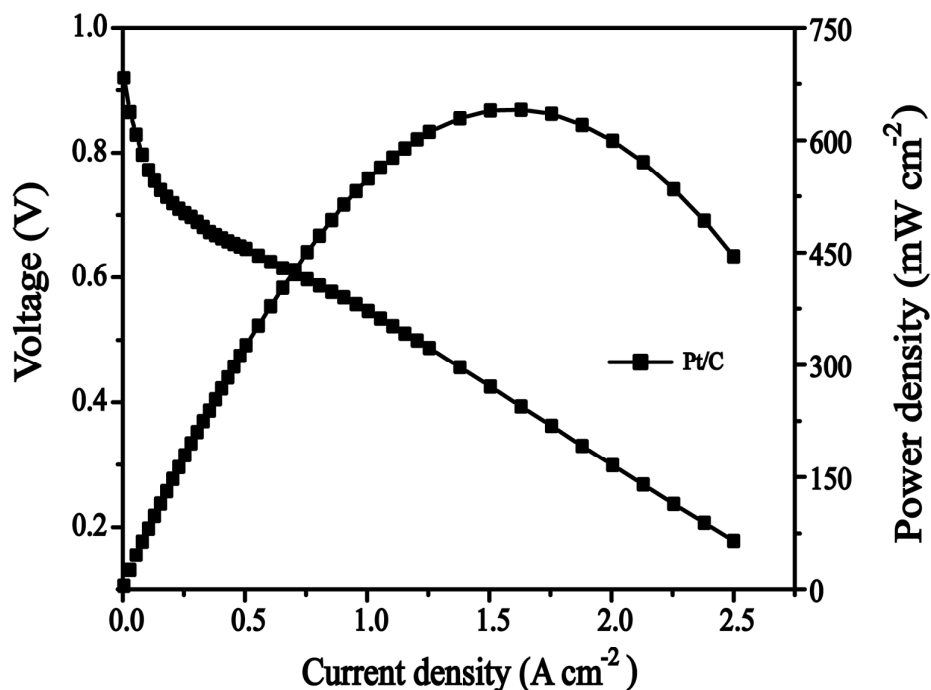


Figure S15. TEM images of FeGNT after ADT in (a) 0.1 M HClO<sub>4</sub>, (b) 0.5 M H<sub>2</sub>SO<sub>4</sub> and (c) 0.1 M KOH.



**Figure S16.** Single cell polarization plots recorded (active area is 4 cm<sup>2</sup>) at 65 °C of a PEMFC with 0.5 mg cm<sup>-2</sup> of Pt/C on both anode and cathode with Nafion 212 as the proton conducting membrane. H<sub>2</sub> and O<sub>2</sub> were used as the fuel and oxidant with flow rates of 50 sccm and 100 sccm, respectively without applying any back pressure.

## References

1. Singh, K. P.; Bae, E. J.; Yu, J.-S., Fe-P: A New Class of Electroactive Catalyst for Oxygen Reduction Reaction. *J. Am. Chem. Soc.* **2015**, *137*, 3165-3168.
2. Lin, L.; Zhu, Q.; Xu, A.-W., Noble-Metal-Free Fe-N/C Catalyst for Highly Efficient Oxygen Reduction Reaction under Both Alkaline and Acidic Conditions. *J. Am. Chem. Soc.* **2014**, *136*, 11027-11033.
3. Bezerra, C. W. B.; Zhang, L.; Lee, K.; Liu, H.; Zhang, J.; Shi, Z.; Marques, A. L. B.; Marques, E. P.; Wu, S.; Zhang, J., Novel Carbon-Supported Fe-N Electrocatalysts

Synthesized Through Heat Treatment of Iron Tripyridyl Triazine Complexes for the PEM Fuel Cell Oxygen Reduction Reaction. *Electrochim. Acta* **2008**, *53*, 7703-7710.

4. Zhao, Y.; Watanabe, K.; Hashimoto, K., Self-Supporting Oxygen Reduction Electrocatalysts Made from a Nitrogen-Rich Network Polymer. *J. Am. Chem. Soc.* **2012**, *134*, 19528-19531.

5. Serov, A.; Artyushkova, K.; Atanassov, P., Fe-N-C Oxygen Reduction Fuel Cell Catalyst Derived from Carbendazim: Synthesis, Structure, and Reactivity. *Adv. Energy Mater.* **2014**, *4*, DOI:10.1002/aenm.201301735.

6. Yang, W.; Liu, X.; Yue, X.; Jia, J.; Guo, S., Bamboo-like Carbon Nanotube/Fe<sub>3</sub>C Nanoparticle Hybrids and Their Highly Efficient Catalysis for Oxygen Reduction. *J. Am. Chem. Soc.* **2015**.

7. Zhou, M.; Yang, C.; Chan, K.-Y., Structuring Porous Iron-Nitrogen-Doped Carbon in a Core/Shell Geometry for the Oxygen Reduction Reaction. *Adv. Energy Mater.* **2014**, *4*, DOI: 10.1002/aenm.201400840.

8. Li, Y.; Zhou, W.; Wang, H.; Xie, L.; Liang, Y.; Wei, F.; Idrobo, J.-C.; Pennycook, S. J.; Dai, H., An Oxygen Reduction Electrocatalyst Based on Carbon Nanotube-Graphene Complexes. *Nat. Nanotechnol.* **2012**, *7*, 394-400.

9. Bianco, G. V.; Losurdo, M.; Giangregorio, M. M.; Capezzuto, P.; Bruno, G., Exploring and Rationalising Effective n-Doping of Large Area CVD-Graphene by NH<sub>3</sub>. *Phys. Chem. Chem. Phys.* **2014**, *16*, 3632-3639.

10. Hu, T.; Sun, X.; Sun, H.; Xin, G.; Shao, D.; Liu, C.; Lian, J., Rapid Synthesis of Nitrogen-Doped Graphene for a Lithium Ion Battery Anode with Excellent Rate Performance and Super-Long Cyclic Stability. *Phys. Chem. Chem. Phys.* **2014**, *16*, 1060-1066.